Slowinski, P., Krauskopf, B., & Wieczorek, S. (2008). Mode structure of a semiconductor laser with feedback from two external filters.

Mode structure of a semiconductor laser with feedback from two external filters

P. Słowiński [a], B. Krauskopf [a], S. Wieczorek [b]

[a]Department of Engineering Mathematics, University of Bristol, UK
[b]School of Engineering, Computing and Mathematics, University of Exeter, UK

ABSTRACT

We study a semiconductor laser subject to filtered optical feedback from two separate filters. This work is motivated by an application where two fiber gratings are used to stabilize the output of a laser source. Specifically, we consider the structure of the external filtered modes (EFMs), which are the basic cw-states of the system. The system is modelled by a set of four delay differential equations with two delays that are due to the travel times of the light in each of the external cavities. Here, each filter is approximated by a Lorentzian and we assume that there is no interaction between the two filters.

We derive a transcendental equation for the EFMs as a function of the widths, detunings and the feedback strengths of the two filters. With continuation techniques we investigate how the number of EFMs changes with parameters. In particular, we consider the equation for its envelope. This allows us to determine regions in the plane of the two detunings that correspond to one, two or three EFM components — disjoint closed curves that are traced out by the EFMs as a function of the feedback phase.

Keywords: semiconductor laser, filtered feedback, external filtered modes

1. INTRODUCTION

Semiconductor lasers are very sensitive to the influence of external optical feedback, and stabilizing them has always been an important issue. It has been shown that filtered optical feedback (FOF) can improve the laser performance.[1,2] On the other hand, the influence of FOF on the laser can lead to other complicated dynamics.[3,4]

External cavities created by feedback loops allow the laser to operate at various compound-cavity modes (continuous wave solutions or cw-states). For the single FOF laser, they are also called external filtered modes (EFMs), in analogy with the external cavity modes (ECMs) of the laser subject to conventional optical feedback (COF). It has been shown that EFMs lie on closed curves in the $(\omega_s,\, N_s)$-plane, which are called the EFM-components.[5] The EFM-components have the form of an ellipse in the $(\omega_s,\, N_s)$-plane that is distorted by the influence of the filter profile. They are traced out by the EFMs as the feedback phase C_p (of the electromagnetic field of the filter, relative to the field of the laser) is varied. A detailed analysis of the dependence of the number of EFM-components on the filter width Λ and the filter detuning Δ (from the laser frequency) was performed in Ref. [6]. It shows that in the $(\Lambda,\, \Delta)$-space there is a region with two EFM-components. A stability and bifurcation analysis of EFMs in Ref. [7] shows that a single FOF laser is very sensitive to changes in feedback phase C_p. Furthermore, the filter parameters (width Λ and detuning Δ) have a big influence on the possible dynamics.[8,9] In a single FOF laser one can observe the well-known relaxation oscillations, but also the frequency oscillations where the frequency of the laser oscillates while its intensity remains almost unchanged.[10] An experimental study of the influence of a feedback phase and a filter detuning on the single FOF laser dynamics can be found in Ref. [8]. The limiting cases of small and big Λ and Δ were presented in Refs. [5, 6, 11].

In this work we study a semiconductor laser subject to FOF from two filter loops (2FOF). The second filter gives an extra set of control parameters, which can give additional control over the laser output. For simplicity we disregard all interactions between the filters. We assume that both filters have the same Lorentzian profile with the filter widths $\Lambda = \Lambda_1 = \Lambda_2$. Moreover, feedback rates κ_1 and κ_2 as well as delay times τ_1 and τ_2 are set equal for both filter loops, that is $\kappa = \kappa_1 = \kappa_2$, $\tau = \tau_1 = \tau_2$. In spite of these assumptions, the second filter significantly influences the dynamics of a laser unit. In the 2FOF system maximally three EFM-components can appear: one around the solitary laser frequency, and the other two around the two filter detuning frequencies. With the tool of numerical continuation it is possible to determine

Send correspondence to P. Słowiński. E-mail: piotr.slowinski@bristol.ac.uk.

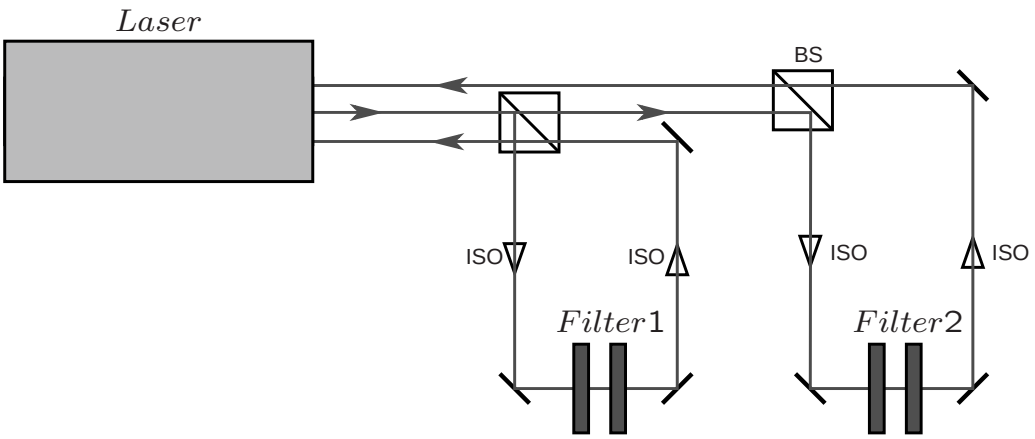

Figure 1. Sketch of a semiconductor laser with feedback from two Fabry-Pérot filter loops; other elements are beam splitters (BS) and optical isolators (ISO).

regions in the (Δ_1, Δ_2)-plane where the 2FOF laser system has one, two or three EFM-components. We show that, as Λ increases, the regions with more than one EFM-components shrink and finally disappear. This is consistent with the fact that, as $\Lambda \rightarrow \infty$, the system reduces to the COF laser. However, a detailed comparison with a laser with two COF loops is beyond the scope of this paper.

2. MATHEMATICAL MODEL

Figure 1 shows a sketch of the 2FOF laser. The optical isolators ensure that there is no COF back to the laser and that there are no interactions between the filters and the laser. The system can be described by rate equations for the complex optical field E inside of the laser, the population inversion N of the laser, and two complex optical fields F_1 and F_2 of the filters. Equations written in the frame of reference of a fixed solitary laser frequency take the dimensionless form:

$$\frac{dE}{dt} = (1+i\alpha)N(t)E(t) + \kappa_1 F_1(t) + \kappa_2 F_2(t), \tag{1}$$

$$T\frac{dN}{dt} = P - N(t) - (1+2N(t))|E(t)|^2, \tag{2}$$

$$\frac{dF_1}{dt} = \Lambda_1 E(t-\tau_1)e^{-iC_p^1} + (i\Delta_1 - \Lambda_1)F_1(t), \tag{3}$$

$$\frac{dF_2}{dt} = \Lambda_2 E(t-\tau_2)e^{-iC_p^2} + (i\Delta_2 - \Lambda_2)F_2(t). \tag{4}$$

The parameter values for Eqs. (1)–(4) are given in Table 1, and are in the range used in Ref. [6, 7]. The feedback terms $\kappa_1 F_1(t)$ and $\kappa_2 F_2(t)$, with the feedback rates κ_1 and κ_2, model the coupling of the filter fields with the laser field. The feedback phases C_p^1 and C_p^2 in Equations (3) and (4) represent the phase relationship between the laser and filters fields. Throughout our analysis, laser chip parameters including the linewidth enhancement factor α, the carrier decay rate T and the pump parameter P are kept fixed at physically realistic values.

Parameter	Meaning	Value
α	linewidth enhancement factor	5
T	carrier lifetime$\times$photon decay rate	100
P	pump parameter	3.5
$\tau = \tau_1\tau_2$	external cavity round-trip times	500
$\kappa = \kappa_1 = \kappa_2$	feedback rates	0.506
C_p^1, C_p^2	feedback phases	0.0
Δ_1, Δ_2	filter detunings	from 0.0 to 0.7
Λ, Λ_1, Λ_2	filter widths	0.0, 0.015, 0.05 and 0.095

Table 1. System parameters.

Equations (1)–(4) are invariant under the exchange of the two filters, that is, under the exchange of subscripts 1 and 2. The feedback phases C_p^1 and C_p^2 are (translationally) symmetrical under a shift of 2π. Moreover, the system has an S^1-symmetry in common with other optical feedback systems of Lang-Kobayashi type,[3] given by the simultaneous rotations of E, F_1 and F_2.[12,13] Obviously, setting one of the feedback rates to zero, either $\kappa_1 = 0$ or $\kappa_2 = 0$, reduces the 2FOF laser to the single FOF laser. Furthermore, setting the same parameters (Λ, Δ, τ, C_p) for both filters also reduces system (1)–(4) to a single FOF laser with feedback rate $\kappa = \kappa_1 + \kappa_2$.

Equations (1)–(4) are a system of delay differential equations (DDEs) with two constant fixed delays τ_1 and τ_2. Hence, its phase space is the infinite-dimensional space of continuous functions over the maximal delay interval with values in (E, N, F_1, F_2)-space. This makes the analysis of DDEs quite challenging. Fortunately, the stability and bifurcation theory for DDEs with fixed delays is well developed[14] and there are well-established numerical continuation tools[15] for the bifurcation analysis of DDEs.

3. EXTERNAL FILTER MODES

Mathematically, an EFM is a group orbit of the S^1-symmetry in (E, N, F_1, F_2)-space. Physically, an EFM has constant intensity, inversion and frequency, and is given by

$$(E(t), N(t), F_1(t), F_2(t)) \quad = \quad \left(E_s e^{i\omega_s t}, N_s, F_s^1 e^{i(\omega_s t+\phi_1)}, F_s^2 e^{i(\omega_s t+\phi_2)}\right). \tag{5}$$

Here, E_s, F_s^1 and F_s^2 are fixed real values of the field amplitude of the laser field and both filtered fields, N_s is a fixed level of inversion, ω_s is a fixed frequency, and ϕ_1, ϕ_2 are fixed phase shifts between the laser field and filtered fields.

3.1 Transcendental equation

To find EFMs, we substitute (5) into Eqs. (1)–(4). Equating real and imaginary parts[6,13] results in the equation:

$$T(\omega_s) = -\omega_s - \sqrt{1+\alpha^2}\left(\frac{\kappa_1\Lambda_1 \sin(-\phi_1 + \arctan(\alpha))}{\sqrt{{\Lambda_1}^2 + (\omega_s - \Delta_1)^2}} + \frac{\kappa_2\Lambda_2 \sin(-\phi_2 + \arctan(\alpha))}{\sqrt{{\Lambda_2}^2 + (\omega_s - \Delta_2)^2}}\right), \tag{6}$$

where,

$$\begin{aligned} \phi_1 &= -\omega_s\tau_1 - C_p^1 - \arctan\left(\frac{\omega_s - \Delta_1}{\Lambda_1}\right), \\ \phi_2 &= -\omega_s\tau_2 - C_p^2 - \arctan\left(\frac{\omega_s - \Delta_2}{\Lambda_2}\right). \end{aligned} \tag{7}$$

Equation (6) is a transcendental equation for the frequencies of the EFMs. In Eq. (6) the terms in parentheses derive from the first and the second filter. If one of them is set to zero, then Eq. (6) reduces to the transcendental equation from Ref. [6]

for the frequencies of EFMs of the single FOF laser. To find the frequencies ω_s Eq. (6) needs to be solved numerically. Once ω_s is known, the values of the other state variables of the EFMs can be found as:

$$N_s = -\left(\frac{\kappa_1\Lambda_1\cos(\phi_1)}{\sqrt{{\Lambda_1}^2+(\omega_s-\Delta_1)^2}}+\frac{\kappa_2\Lambda_2\cos(\phi_2)}{\sqrt{{\Lambda_2}^2+(\omega_s-\Delta_2)^2}}\right) \tag{8}$$

$$E_s = \sqrt{\frac{P-N_s}{1+2N_s}}, \tag{9}$$

$$F_s^1 = \frac{E_s\Lambda_1}{\sqrt{{\Lambda_1}^2+(\omega_s-\Delta_1)^2}}, \tag{10}$$

$$F_s^2 = \frac{E_s\Lambda_2}{\sqrt{{\Lambda_2}^2+(\omega_s-\Delta_2)^2}}. \tag{11}$$

It can be seen, that equations (8)–(12), like Eqs. (1)–(4), can be reduced to equations for a EFMs state variables for the single FOF laser. For example, it is enough to put $\Lambda_2 = 0$. We have already remarked that for a single FOF laser, the EFMs lie on a curve that is a function of the feedback phase C_p. In case of two filtered feedback loops we are dealing with a surface of EFMs which is a function of C_p^1 and C_p^2. The EFM-components are sections of that surface for a set value of C_p^1 or C_p^2.

Following Ref. [6], we know that the number of EFM-components corresponds to the number of intervals given by roots of the envelope of Eq. (6), which changes when we vary the filter width or the filter detuning. The envelope of Eq. (6) is obtained as the maximal and minimal values of ±1 of the sine functions in Eq. (6). The values of ω_s for both parts of envelope of Eq. (6) can be found as roots of the equation:

$$\begin{aligned} F(\omega_s) = {\omega_s}^2({\Lambda_1}^2+(\omega_s-\Delta_1)^2)({\Lambda_2}^2+(\omega_s-\Delta_2)^2) \\ -\left(\kappa_1\Lambda_1\sqrt{{\Lambda_1}^2+(\omega_s-\Delta_1)^2}+\kappa_2\Lambda_2\sqrt{{\Lambda_2}^2+(\omega_s-\Delta_2)^2}\right)^2(1+\alpha^2). \end{aligned} \tag{12}$$

Similarly to system (1)–(4), equation (12) can be reduced to the equivalent equation for the single FOF laser. However, because of a term with square roots in Eq. (12), unlike in the case of FOF, the derivation of simple analytical expressions for the parametrisation of regions with different number of EFM-components in the $(\Lambda_1,\, \Lambda_2,\, \Delta_1,\, \Delta_2)$-space does not follow.

Figure 2 shows regions (grey) of negative values of Eq. (12) in projection onto the $(\omega_s,\, \Delta_1)$-plane. Here we fixed $\Delta_2 = 0.15$, $\Lambda = 0.015$ for values of the other parameters as given in Table 1. Negative values of Eq. (12) are bounded by its roots. Shaded intervals on the ω_s-axis, located in between these roots, correspond to separate EFM-components. It can be seen that indeed the maximal number of EFM-components for the given parameter set is three. One of the minima of function $F(\omega_s)$ is always around the solitary laser frequency $\omega_s = 0$, the second is around the detuning frequency of the second filter $\omega_s = 0.15$, and the third is moving from left to right as the detuning frequency of the first filter is increased. We can observe that, when Δ_1 increases, the number of EFM-components changes. First it changes from two to three at approximately $\Delta_1 = -0.34$, next it decreases to two again, and then to one around $\Delta_1 = 0$. As Δ_1 further increases, so does the number of EFM-components: it is two around $\Delta_1 = 0.25$, then three and finally it settles back at two for $\Delta_1 > 0.34$. The black dots in Fig. 2 are turning points of $F(\omega_s)$ with respect to Δ_1, see section 3.3.

3.2 EFM-components

Figure 3 shows EFMs in the $(\omega_s,\, N_s)$-plane. They are the solutions of Eqs. (6)–(11) and trace out the grey curves as function of the feedback phase of the filters where $C_p^1 = C_p^2$. Black dots show the positions of the EFMs for $C_p^1 = C_p^2 = 0$. These curves were found by continuation of the full system (1)–(4) in the continuation parameters C_p^1 and ω_s, under the

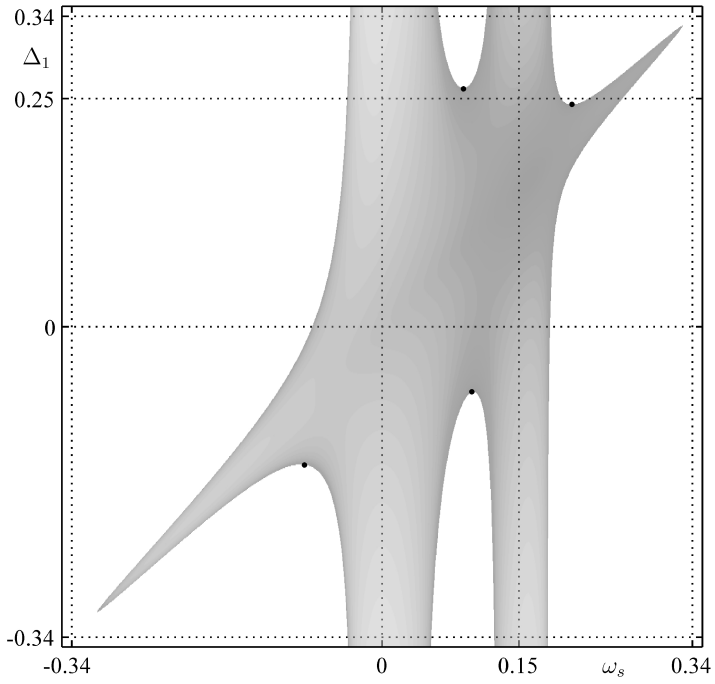

Figure 2. Regions of negative values of Eq. (12) for $\Delta_1 \in [-0.35, 0.35]$, $\Delta_2 = 0.15$ and $\Lambda = 0.015$.

condition that $C_p^1 = C_p^2$. In Fig. 3 (a), when $\Delta_1 = \Delta_2 = 0$, there is a single group of EFMs around the solitary frequency of the laser. Panel (b) shows that for $\Delta_1 = -0.12$ and $\Delta_2 = 0$, a second group of EFMs appears around the changed filter detuning frequency. Panel (c) is almost the π-rotation of panel (b) and was obtained by changing the sign of Δ_1. Finally, when we change both filter detunings to $\Delta_1 = -0.12$ and $Delta_2 = 0.12$, three groups of EFMs appear: the first and the second around the two filter detuning frequencies, and the third around the solitary laser frequency. In accordance with Fig. 2, as we vary the filter detunings, EFMs are forming one, two or three components.

Note that in Fig. 3 (d) the EFM-component around the solitary laser frequency is substantially smaller than the two other EFM-components. This results from the interference between the two sine terms in Eq. (6). The insert shows that this EFM-component has a shape similar to the ellipse found for a COF laser. This shape of the EFM-component is a result of the feedback from highly detuned filters modelled by relatively flat tails of the filter profiles. Consequently all frequencies around the solitary laser frequency are fed back with approximately the same very low feedback strength. This resembles the effect of weak COF.[16]

3.3 The number of EFM-components

Throughout this section we study the maximal number of EFM-components. While the actual number of EFM-components depends on $\Lambda, \Delta, \kappa, \tau$ and C_p, the envelope of transcendental equation is not dependent on the feedback phase C_p or the delay time τ. In fact, the envelope of transcendental equation gives conditions for the maximal possible number of EFM-components. All calculations that follow have been performed for $C_p^1 - C_p^2 = 0$. Taking into consideration the dependence of the envelope on other parameters of the system is beyond the scope of this paper.

Equation (12) is parametrised by Δ_1, Δ_2, Λ_1 and Λ_2. To determine regions in the (Δ_1, Δ_2)-plane with different maximal numbers of EFM components, we numerically solved Eq. (12) and its derivative with respect to ω_s. Points for which $F(\omega_s) = 0$ and $\frac{dF(\omega_s)}{d\omega_s} = 0$ are shown in Fig. 2 as black dots. Note that solving the equation for the envelope of Eq. (6) and its derivative with respect to ω_s gives the same results. To obtain solutions for different values of Δ_1 and Δ_2, we solved $F(\omega_s)$ and $\frac{dF(\omega_s)}{d\omega_s}$ by means of numerical continuation with the MATLAB package DDE-BIFTOOL.[17]

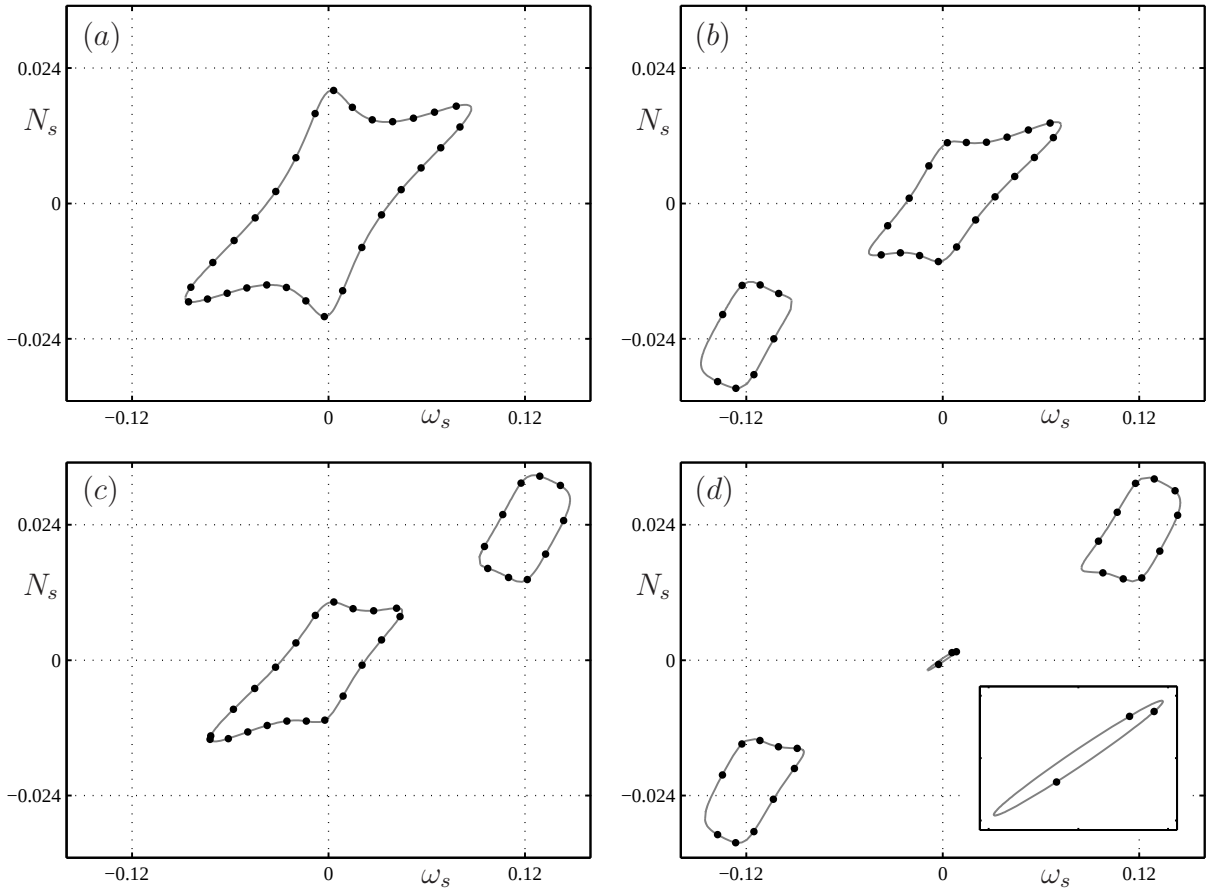

Figure 3. Curves of EFMs in the (ω_s, N_s)-plane obtained by continuation. Black dots correspond to the discrete set of EFMs for $C_p^1 = C_p^2 = 0$ and $\Lambda = 0.015$. Shown are the cases of a single EFM-component for $\Delta_1 = \Delta_2 = 0$ (a), two EFM-components for $\Delta_1 = -0.12$, $\Delta_2 = 0$ (b), two EFM-components for $\Delta_1 = 0.12$, $\Delta_2 = 0$ (c) and three EFM-components for $\Delta_1 = 0.12$, $\Delta_2 = -0.12$ (d).

Figure 4 shows regions in the (Δ_1, Δ_2)-plane with maximally one, two or three EFM-components (as denoted by numbers). The grey curves are the result of numerical continuation, and they bound regions with different numbers of EFM-components, typically two of them. The intersection of two regions with maximally two EFM-components gives rise to a region with maximally three EFM-components: one common EFM-component around the solitary laser frequency and one component around each of the filter frequencies. The different panels show how increasing the filter width changes the dependence of the maximal number of EFM-components on the filter detunings. As we have already remarked, we only analysed the case when both filters have the same profile, that is $\Lambda = \Lambda_1 = \Lambda_2$. Figure 4 (a) shows the degenerate case for $\Lambda = 0$ with no EFM-components. In all regions in panel (a) marked by 0, as well as at the point $\Delta_1 = \Delta_2 = 0$, there is only one EFM at the solitary laser frequency. Maximally two single EFMs can be found only for cases $\Delta_1 = 0$ or $\Delta_2 = 0$ (vertical and horizontal lines), or $\Delta_1 = \Delta_2$ (diagonal). This picture changes dramatically when Λ is increased. In panel (b) for $\Lambda = 0.015$ regions with different maximal number of EFM-components form a very regular pattern. It is mainly the result of a very fast growth of the region with one EFM-component around the solitary laser frequency. This region originates from the point where $\Delta_1 = \Delta_2 = 0$. The growth of this area when Λ is increased, means that regions with three EFM-components shrink and some of them disapear; see panel (c) for $\Lambda = 0.05$. Figure 4 (d) for $\Lambda = 0.095$ shows that, when Λ is increased, all regions with three EFM-components disappear and regions with two EFM-components shrink even further. For $\Lambda \to \infty$ the 2FOF laser reduces to a laser subject to a single COF (note that the COF laser does not depend on Δ). This agrees with the observation that for sufficiently large Λ, there is only a single EFM-component.

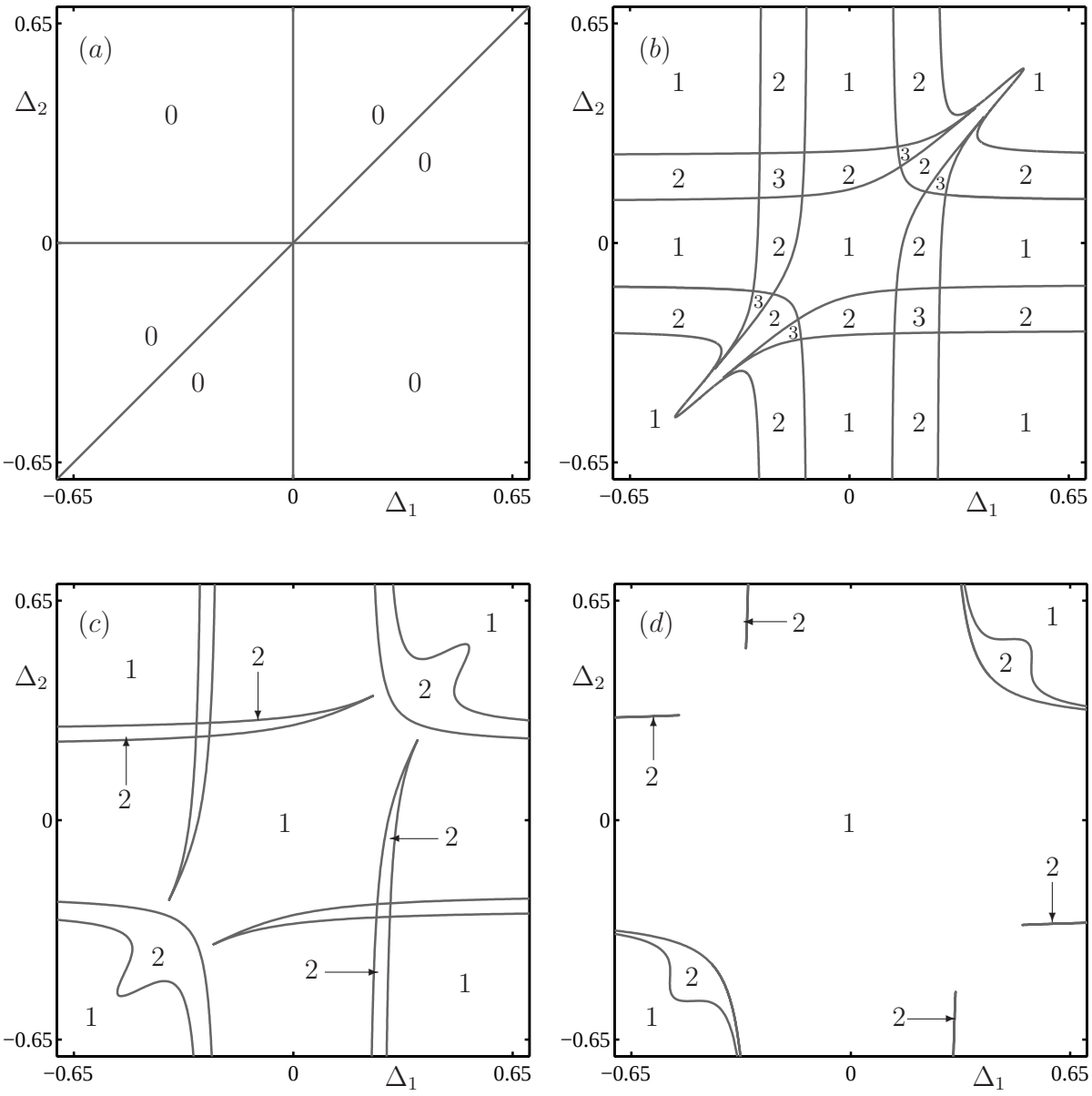

Figure 4. Regions in the $(\Delta_1,\, \Delta_2)$-plane with a single EFM solution (0), a single EFM-component (1), two isolated EFM-components (2), and three isolated EFM-components (3). Panels (a)–(d) show the dependence of these regions on the filter width $\Lambda = \Lambda_1 = \Lambda_2$; from (a) to (d) Λ takes values $\Lambda = 0$, $\Lambda = 0.015$, $\Lambda = 0.05$ and $\Lambda = 0.095$.

4. CONCLUSIONS

We have presented a study of the EFM structure of a semiconductor laser subject to two FOF loops. Our results show that the presence of the second filter loop significantly influences the laser output. We showed how the maximal number of EFM-components depends on filter detunings Δ and the filter width Λ. To this end, we presented the transcendental equation for frequencies of EFMs and analytical expressions for the other state variables of EFMs. With the tool of numerical continuation we showed that a 2FOF laser can have maximally three EFM-components. Furthermore, we studied how regions with different maximal numbers of EFM-components in the $(\Delta_1,\, \Delta_2)$-plane depend on Λ. A more detailed

analysis of the dependence of the number of EFM-components on the other parameters, as well as a stability and bifurcation analysis of EFMs of the 2FOF laser are the subject of ongoing research.

REFERENCES

1. A. Fischer, M. Yousefi, D. Lenstra, M. Carter, and G. Vemuri, "Experimental and theoretical study of semiconductor laser dynamics due to filtered optical feedback," *IEEE Journal of Selected Topics in Quantum Electronics* **10 (5)**, pp. 944–954, 2005.
2. B. Dahmani, L. Hollberg, and R. Drullinger, "Frequency stabilization of semiconductor lasers by resonant optical feedback," *Opt. Lett.* **12**(11), pp. 876–878, 1987.
3. R. Lang and K. Kobayashi, "External optical feedback effects on semiconductor injection laser properties," *IEEE Journal of Quantum Electronics* **16 (3)**, pp. 347–355, 1980.
4. M. Yousefi, D. Lenstra, A. Fischer, and G. Vemuri, "Simulations of a semiconductor laser with filtered optical feedback: deterministic dynamics and transitions to chaos," in *Physics and Simulation of Optoelectronic Devices X*, P. Blood, M. Osinski, and Y. Arakawa, eds., *Proceedings of SPIE* **4646**, pp. 447–452, 2002.
5. M. Yousefi and D. Lenstra, "Dynamical behavior of a semiconductor laser with filtered external optical feedback," *IEEE J. Quantum Electron.* **35 (6)**, pp. 970–976, 1999.
6. K. Green and B. Krauskopf, "Mode structure of a semiconductor laser subject to filtered optical feedback," *Opt. Comm.* **258 (2)**, pp. 243–255, 2006.
7. H. Erzgräber, B. Krauskopf, and D. Lenstra, "Bifurcation analysis of a semiconductor laser with filtered optical feedback," *SIAM J. Appl. Dyn. Sys.* **6 (1)**, pp. 1–28, 2006.
8. H. Erzgräber, D. Lenstra, B. Krauskopf, A. P. A. Fischer, and G. Vemuri, "Feedback phase sensitivity of a semiconductor laser subject to filtered optical feedback: experiment and theory," *Physical Review E* **76 (2)**, 2007.
9. H. Erzgräber and B. Krauskopf, "Dynamics of a filtered-feedback laser: influence of the filter width," *Optics Letters* **32 (16)**, pp. 2441–2443, 2007.
10. A. Fischer, M. Yousefi, D. Lenstra, M. Carter, and G. Vemuri, "Filtered optical feedback induced frequency dynamics in semiconductor lasers," *Phys. Rev. Lett.* **92**, p. 023901, Jan 2004.
11. G. Hek and V. Rottschäfer, "Semiconductor laser with filtered optical feedback: from optical injection to conventional feedback," *IMA J Appl Math* **72**(4), pp. 420–450, 2007.
12. B. Krauskopf, "Bifurcation analysis of lasers with delay," in *Unlocking Dynamical Diversity: Optical Feedback Effects on Semiconductor Lasers*, D. Kane and K. Shore, eds., pp. 147–183, Wiley, 2005.
13. B. Heageman, K. Engelborghs, D. Roose, D. Pieroux, and T. Erneux, "Stability and rupture of bifurcation bridges in semiconductor lasers subject to optical feedback," *Phys. Rev. E* **66 (4)**, 2002.
14. O. Diekmann, S. A. van Gils, S. M. Verduyn Lunel and H.-O. Walther, *Delay Equations: Functional-, Complex-, and Nonlinear Analysis*, Springer-Verlag, New York, 1995.
15. D. Roose and R. Szalai, "Continuation and bifurcaton analysis of delay differential equations," in *Numerical Continuation Methods for Dynamical Systems, Pathfollowing and boundary value problems*, B. Krauskopf, H. Osinga, and J. Galán-Vioque, eds., pp. 359–399, Springer, Dordrecht, 2007.
16. D. Lenstra and M. Yousefi, "Theory of delayed optical feedback in lasers," in *Fundamental Issues of Nonlinear Laser Dynamics*, B. Krauskopf and D. Lenstra, eds., *AIP Conference Proceedings* **548**, pp. 87–111, (Melville, New York), 2000.
17. K. Engelborghes, T. Luyzanina, and G. Samaey, "DDE-BIFTOOLS v. 2.00 user manual: A Matlab package for bifurcation analysis of delay differential equations, Tech. report tw-330" , Department of Computer Science, K. U. Leuven, 2001.